Histol Histopathol (2023) 38: 73-89

http://www.hh.um.es

Histology and Histopathology
From Cell Biology to Tissue Engineering

ORIGINAL ARTICLE **Open Access**

Circ_0000520 interacts with miR-512-5p to upregulate KIAA0100 to promote malignant behaviors in lung cancer

Linxuan Wang, Wenjing Jin, Xiaochi Wu, Yuan Liu and Wenchao Gu

Department of Respiratory and Critical Care Medicine, Shanghai Pudong New Area People's Hospital, Shanghai, China

Summary. Background. CircRNAs function as pivotal molecules to regulate the malignant development of lung cancer. This study was designed to research the functional role and how it acted in lung cancer progression.

Methods. Circ_0000520, microRNA-512-5p (miR-512-5p) and Breast cancer-overexpressed gene 1 (KIAA0100) levels were measured through reverse transcription-quantitative polymerase chain reaction assay. Cell Counting Kit-8 assay and EdU assay were used to examine cell proliferation. Cell cycle and apoptosis were evaluated via flow cytometry. The protein levels were determined using western blot. Cell migration and invasion were assessed by wound healing assay and transwell assay. The circ_0000520 function *in vivo* was explored by tumor xenograft assay. The molecular interaction was analyzed via Dual-luciferase reporter assay.

Results. Circ_0000520 was obviously upregulated in lung cancer tissues and cells. Silence of circ_0000520 inhibited proliferation, cell cycle progression, migration, invasion and angiogenesis but promoted cell apoptosis. Circ_0000520 downregulation reduced tumor growth of lung cancer *in vivo*. Circ_0000520 served as a miR-512-5p sponge. The oncogenic function of circ_0000520 was partly achieved by sponging miR-512-5p in lung cancer. KIAA0100 was a target of miR-512-5p and miR-512-5p inhibited the malignant behaviors of lung cancer cells via downregulating KIAA0100. Circ_0000520 targeted miR-512-5p to regulate the level of KIAA0100.

Conclusion. All these data demonstrated that circ_0000520 was able to drive the progression of lung cancer via the mediation of miR-512-5p/KIAA0100 axis. Circ_0000520 might be a potential biomarker for lung cancer.

Corresponding Author: Wenchao Gu, Department of Respiratory and Critical Care Medicine, Shanghai Pudong New Area People's Hospital, No. 490 Chuanhuan South Road, Pudong New Area, Shanghai 201200, China. e-mail: guwenchao2018@163.com

DOI: 10.14670/HH-18-498

Key words: circ_0000520, miR-512-5p, KIAA0100, Lung cancer

Introduction

Lung cancer remains one of the most frequently malignant tumors with high morbidity and mortality rates per year (Thai et al., 2021). Patients are usually diagnosed at an advanced stage because of poor diagnosis at early-stage (Nooreldeen and Bach, 2021). In addition, tumor metastasis is an important cause of treatment failure and cancer recurrence (Xie et al., 2021). Increasing biomolecules have been found to drive tumorigenesis and development in lung cancer, and targeted therapies have been used for clinical treatment (Halliday et al., 2019). Thus, exploring the molecular mechanism in occurrence and metastasis of lung cancer is necessary.

Circular RNAs (circRNAs) and microRNAs (miRNAs) have biological significance in lung cancer progression (Drula et al., 2020). More interestingly, circRNAs lead to gene regulation by sponging miRNAs in various cancers (Panda, 2018). Circ_0000520 was indicated to promote cell growth and metastasis of breast cancer via increasing ZFX level through absorbing miR-1296 (Zhou et al., 2021; Zheng et al. 2021) declared that circ_0000520 enhanced proliferation ability of cervical cancer cells by the miR-1296/CDK2 axis (Zheng et al., 2021), and Sun et al. reported that circ_0000520 targeted the different miRNA/mRNA networks to participate in the malignant behaviors of gastric cancer Sun et al. (2018). The involvement of circ_0000520 in lung cancer is not clear. miRNAs are implicated in the pathogenesis of lung cancer via negatively regulating the level of genes (Zarredar et al., 2018). MicroRNA-512-5p (miR-512-5p) acted as a tumor repressor in lung cancer via targeting p21 and β-catenin (Chu et al., 2016; Wang et al., 2020c). Breast cancer-overexpressed gene 1 (BCOX1, KIAA0100) has been validated as an oncogene in breast cancer and prostate cancer (Liu et al., 2014; Guo et al., 2015). Whether KIAA0100 plays a

carcinogenic role in lung cancer is unreported. Also, the target relation between miR-512-5p and KIAA0100 remains to be researched.

Moreover, the potential of circ_0000520 to regulate the level of KIAA0100 via targeting miR-512-5p was explored. The purposes of this study were to ascertain the biological function and regulatory mechanism of circ_0000520 in the malignant development of lung cancer.

Materials and methods

Human sample collection

46 patients were diagnosed with lung cancer by two experienced pathologists at Shanghai Pudong New Area People's Hospital. These patients have signed the written informed consent forms to participate in this study. The lung cancer tissues (n=46) and the adjacent counterparts (n=46) were collected during surgical resection, then stored at -80°C. All operations on human samples followed the Declaration of Helsinki. This study was authorized by the Ethics Committee of Shanghai Pudong New Area People's Hospital.

Cell culture and transfection

H1299, HCC827, A549 and H460 cell lines were applied for lung cancer research, and 16HBE (human bronchial epithelial cell line) was used as a normal control. All cells were from BioVector NTCC Inc. (Beijing, China), and cultivated at 37°C with 5% CO_2. Cell medium was prepared by Dulbecco's modified eagle medium (DMEM; Hyclone, Logan, UT, USA), 1% penicillin/streptomycin (Sigma, St. Louis, MO, USA) and 10% fetal bovine serum (FBS; Sigma). The short hairpin RNA lentiviral vector for circ_0000520 (sh-circ_0000520), miRNA mimic for miR-512-5p (miR-512-5p), and miRNA inhibitor for miR-512-5p (anti-miR-512-5p), as well as the negative controls (sh-NC, miR-NC, anti-NC) were synthesized by GenePharma (Shanghai, China). KIAA0100 sequence was inserted into the pcDNA vector (Invitrogen, Carlsbad, CA, USA), constructing the pcDNA-KIAA0100 (KIAA0100) for overexpression of KIAA0100. The 96-well plates were seeded with 1×10^4 cells/well, and 70%-confluent cells were transfected with RNAs and vectors via Lipofectamine™ 3000 transfection reagent (Invitrogen).

Reverse transcription-quantitative polymerase chain reaction (RT-qPCR) assay

TransGen (Beijing, China) provided the detection reagents for RT-qPCR assay. TransZol Kit was performed to extract total RNA from tissues and cells, then the complementary DNA (cDNA) was obtained using *EasyScript*® All-in-One First-Strand cDNA Synthesis SuperMix. PCR was then conducted by *TransStart*® Green qPCR SuperMix, according to the instruction book. In addition, total RNA was digested with 4 U/μg RNase R (GENESEED) at 37°C for 2h to assess the RNA stability of circ_0000520 and RPPH1. Also, circ_0000520 localization was analyzed by RT-qPCR after RNA was isolated from nuclear and cytoplasmic fractions through PARIS™ Kit (Invitrogen). Glyceraldehyde-phosphate dehydrogenase (GAPDH) served as a reference gene for circRNA and mRNA, while miRNA level normalization was performed by U6. The primer sequences are exhibited in Table 1. Data were analyzed and calculated via the $2^{-\Delta\Delta Ct}$ method (Livak and Schmittgen, 2001).

Cell Counting Kit-8 (CCK-8) assay

H1299 and A549 cells were performed with transfection for 0 h, 24 h, 48 h or 72 h. After incubation with 10 μL CCK-8 solution (Beyotime, Shanghai, China) for 3 h, the optical density value at 450 nm was determined using a microplate reader and cell curves were produced.

EdU assay

1×10^5 cells/well were planted into the 48-well plates, then cell proliferation was examined through EdU Detection Kit (Beyotime) after transfection for 48 h. Briefly, cells were labeled with EdU solution and cell nuclei were stained with diamidine phenylindole (DAPI; Beyotime). Cell detection was carried out under the fluorescence microscope (Olympus, Tokyo, Japan) to distinguish the EdU-positive cells (EdU+DAPI).

Cell cycle assay

5×10^5 cells were collected for cell cycle examination using Cell cycle detection kit (Jiancheng Bioengineering Institute, Nanjing, China). Cells were incubated with 1 mL ice-cold ethanol (Beyotime) at -20°C overnight, and then washed with 500 μL phosphate buffer solution

Table 1. Primer sequences used for RT-qPCR.

Name	Primer sequences (5'-3')
circ_0000520	Forward: GGGAAGGTCTGAGACTAGGG Reverse: GGACATGGGAGTGGAGTGAC
miR-512-5p	Forward: GCCGAGCACTCAGCCTTGAG Reverse: GCAGGGTCCGAGGTAT
KIAA0100	Forward: GCTGGGGTGGATCAAAAGGA Reverse: TCCTCCAGCTGACCACTCTT
RPPH1	Forward: GTCACTCCACTCCCATGTCC Reverse: CAGCCATTGAACTCACTTCG
GAPDH	Forward: GACAGTCAGCCGCATCTTCT Reverse: GCGCCCAATACGACCAAATC
U6	Forward: CTCGCTTCGGCAGCACATATACTA Reverse: ACGAATTTGCGTGTCATCCTTGCG

(PBS; Beyotime) and resuspended in 100 μL RNase A solution. Subsequently, cells were added with 400 μL Propidium Iodide (PI) solution at 4°C for 30 min and cell absorbance was measured at 488 nm through a flow cytometer (BD Biosciences, San Diego, CA, USA).

Cell apoptosis assay

The apoptosis assessment was performed by Annexin V-fluorescein isothiocyanate (Annexin V-FITC) Apoptosis Detection Kit (Invitrogen). 6×10^4 cells were harvested after transfection for 72h, then suspended in 1× Binding Buffer. Thereafter, cell suspension was stained with 5 μL Annexin V-FITC for 10 min and 10 μL PI for 5 min away from light. Under the flow cytometer (BD Biosciences), Annexin V+/PI- and Annexin V+/PI+ labeled cells were recognized as the apoptotic cells.

Western blot

Radioimmunoprecipitation assay (RIPA) buffer (Beyotime) was employed for total protein acquisition as per the manufacturer's specification, followed by expression detection as previously described (Li et al., 2021). The primary antibodies are displayed below: proliferating cell nuclear antigen (PCNA; Abcam, Cambridge, UK, ab18197, 1:1000), Cyclin D1 (Abcam, ab16663, 1:1000), Bcl-2 associated X (Bax; Abcam, ab32503, 1:1000), Vimentin (Abcam, ab45939, 1:1000), vascular endothelial growth factor (VEGFA; Abcam, ab52917, 1:1000), KIAA0100 (Invitrogen, PA5-69444, 1:1000), GAPDH (Abcam, ab128915, 1:3000). Goat anti-rabbit IgG H&L (HRP) (Abcam, ab205718, 1:5000) was used as the secondary antibody. Electrochemiluminescence (ECL) reagent (Beyotime) was used for the exhibition of blots, and level analysis was implemented using Image J software (NIH, Bethesda, MD, USA).

Wound healing assay

After 24h of transfection, two straight scratches were produced by a sterile 200 μL pipette tip in H1299 and A549 cells. Cells were washed with 500 μL PBS, then cultured in serum-free medium for 24h. The migration distance (width at 0h – width at 24h) was measured and migration rate was calculated by migration distance/width at 0 h ×100%.

Transwell assay

1×10^5 cells were seeded into the transwell chamber (Corning Inc., Corning, NY, USA) coated with matrigel (BD Biosciences), while 500 μL cell medium was added into the lower chamber. After incubation at 37°C for 24h, the invaded cells were fixated by 4% paraformaldehyde (Beyotime) and stained in 0.1% crystal violet (Beyotime). Cell number was counted in three fields of view by an inverted microscope (Olympus). The images were acquired at 100× magnification.

Tube formation assay

Human Umbilical Vein Endothelial Cells (HUVECs, BioVector NTCC Inc.) were inoculated into 48-well plates coated with 60 μL Matrigel (BD Bioscience). H1299 and A549 cells were co-cultured with HUVECs for 48 h, then the capillary-like branches were counted in 5 random fields through a computer-assisted microscope.

In vivo experiment

1×10^6 sh-circ_0000520 or sh-NC transfected H1299 cells were resuspended in 200 μL PBS, then subcutaneously injected into the flank of BALB/c nude mice (Vital River Laboratory Animal Technology Co., Ltd., Beijing, China) with 5 mice/group. Tumor size was monitored every week, and tumor volume was calculated by length×width^2×0.5. Mice were sacrificed through the inhalation of CO_2 after 28 d, and tumors were dissected from mice. The weight was determined under an electronic scale, followed by circ_0000520 quantification via RT-qPCR. Ki67 (ab15580) protein expression measured by Immunohistochemistry (IHC) assay (Sun et al., 2021). The protocols were ratified by the Animal Ethical Committee of Shanghai Pudong New Area People's Hospital.

Dual-luciferase reporter assay

The sequences of circ_0000520 and KIAA0100 were amplified to be cloned into the pmirGLO plasmid (Promega, Madison, WI, USA). The wild-type (WT) plasmids containing the miR-512-5p binding sites were considered as WT-circ_0000520 and WT-KIAA0100. The mutant plasmids with the mutated miR-512-5p sites were considered as MUT-circ_0000520 and MUT-KIAA0100. H1299 and A549 cells with the co-transfection of circ_0000520 or KIAA0100 plasmid and miR-NC or miR-512-5p were performed at 37°C for 48 h, then Dual-Luciferase Reporter Detection Kit (Promega) was exploited for luciferase activity analysis.

Statistical analysis

Pearson's correlation coefficient was conducted to analyze the linear relationship in lung cancer tissues. Data were collected after experiments were repeated three times, and data are shown as the mean ± standard deviation. SPSS 22.0 (SPSS Inc., Chicago, IL, USA) was applied for data analysis, followed by the comparison of statistical difference through Student's t-test and analysis of variance (ANOVA) followed by Tukey's test. $P<0.05$ showed a significant difference.

Results

Circ_0000520 was highly expressed in lung cancer tissues and cells

GSE158695 dataset has shown that 3 circRNAs (circ_0000517, circ_0000515, circ_0000520) were upregulated in lung cancer samples with log2FC>2.5 and P<0.05 (Fig. 1A). Then, we detected the levels of 3 circRNAs in our 5 paired tissue samples. As depicted in Fig. 1B, the upregulated change of circ_0000520 was the most significant. Thus, circ_0000520 was chosen as a research subject for lung cancer. The expression of circ_0000520 was much higher in 46 lung cancer tissues that in normal controls (Fig. 1C). Also, circ_0000520 was highly expressed in 4 lung cancer cell lines (H1299, HCC827, A549, H460) relative to 16HBE cell line (Fig. 1D). The subsequent assays were performed in H1299 and A549 cells with more obvious upregulation of circ_0000520. RNase R treatment induced the evident inhibition of ribonuclease P RNA component H1 (RPPH1) mRNA level, while it did not influence the circ_0000520 expression in H1299 and A549 cells (Fig. 1E-F). Cell localization analysis demonstrated that circ_0000520 and GAPDH were localized in the cytoplasm while U6 was enriched in the nucleus of H1299 and A549 cells (Fig. 1G-H). The high stability and cytoplasmic localization exhibited the circRNA identification of circ_0000520.

Downregulation of circ_0000520 inhibited proliferation and cell cycle progression but induced apoptosis in lung cancer cells

Relative to sh-NC group, circ_0000520 expression was effectively knocked down in sh-circ_0000520-transfected H1299 and A549 cells while RPPH1 mRNA expression was unchanged (Fig. 2A,B). CCK-8 assay (Fig. 2C,D) and EdU assay (Fig. 2E,F) showed that cell proliferation was inhibited after transfection of sh-circ_0000520, compared with transfection of sh-NC. Flow cytometry indicated that circ_0000520 inhibition

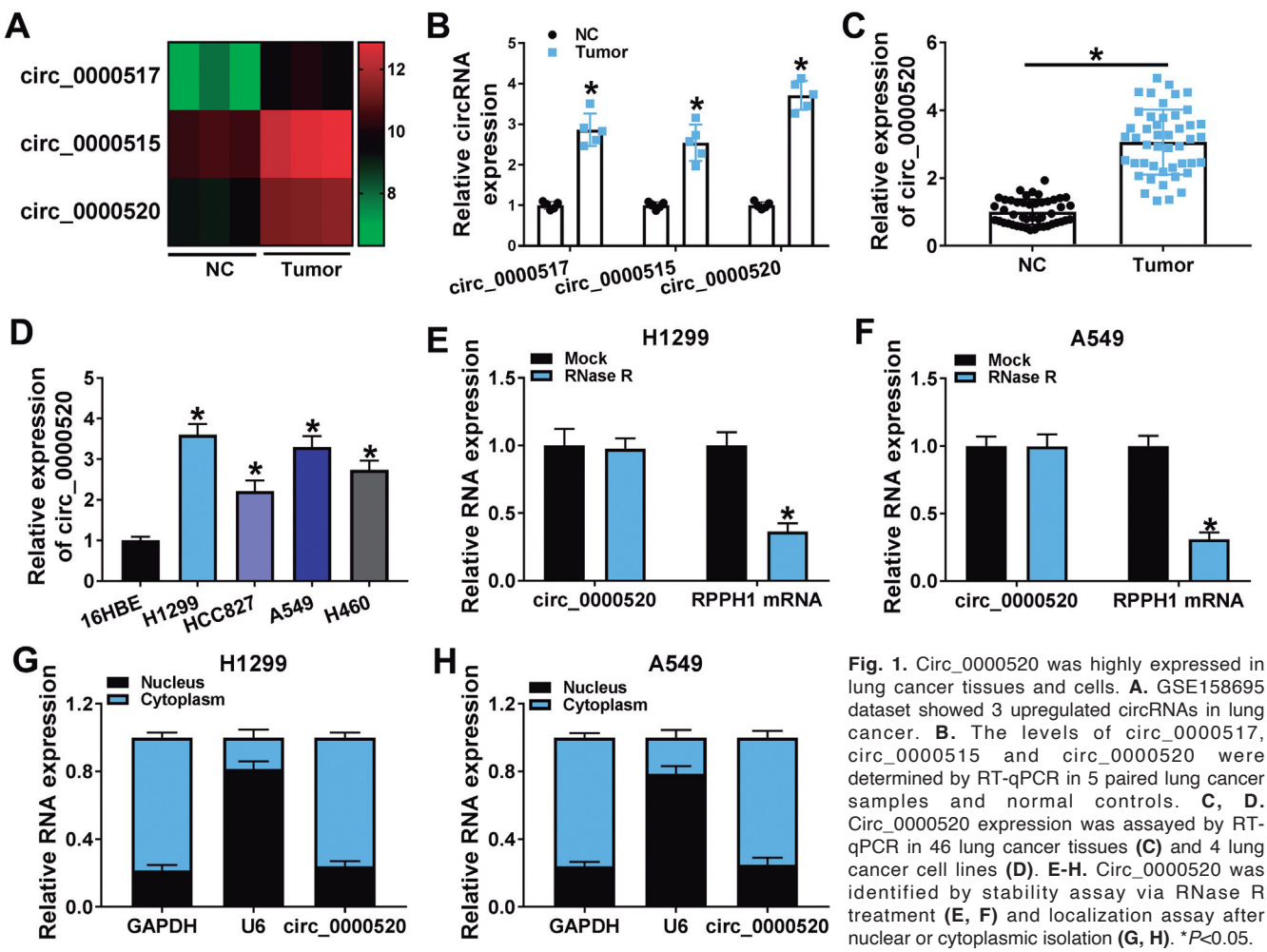

Fig. 1. Circ_0000520 was highly expressed in lung cancer tissues and cells. **A.** GSE158695 dataset showed 3 upregulated circRNAs in lung cancer. **B.** The levels of circ_0000517, circ_0000515 and circ_0000520 were determined by RT-qPCR in 5 paired lung cancer samples and normal controls. **C, D.** Circ_0000520 expression was assayed by RT-qPCR in 46 lung cancer tissues **(C)** and 4 lung cancer cell lines **(D)**. **E-H.** Circ_0000520 was identified by stability assay via RNase R treatment **(E, F)** and localization assay after nuclear or cytoplasmic isolation **(G, H)**. **P*<0.05.

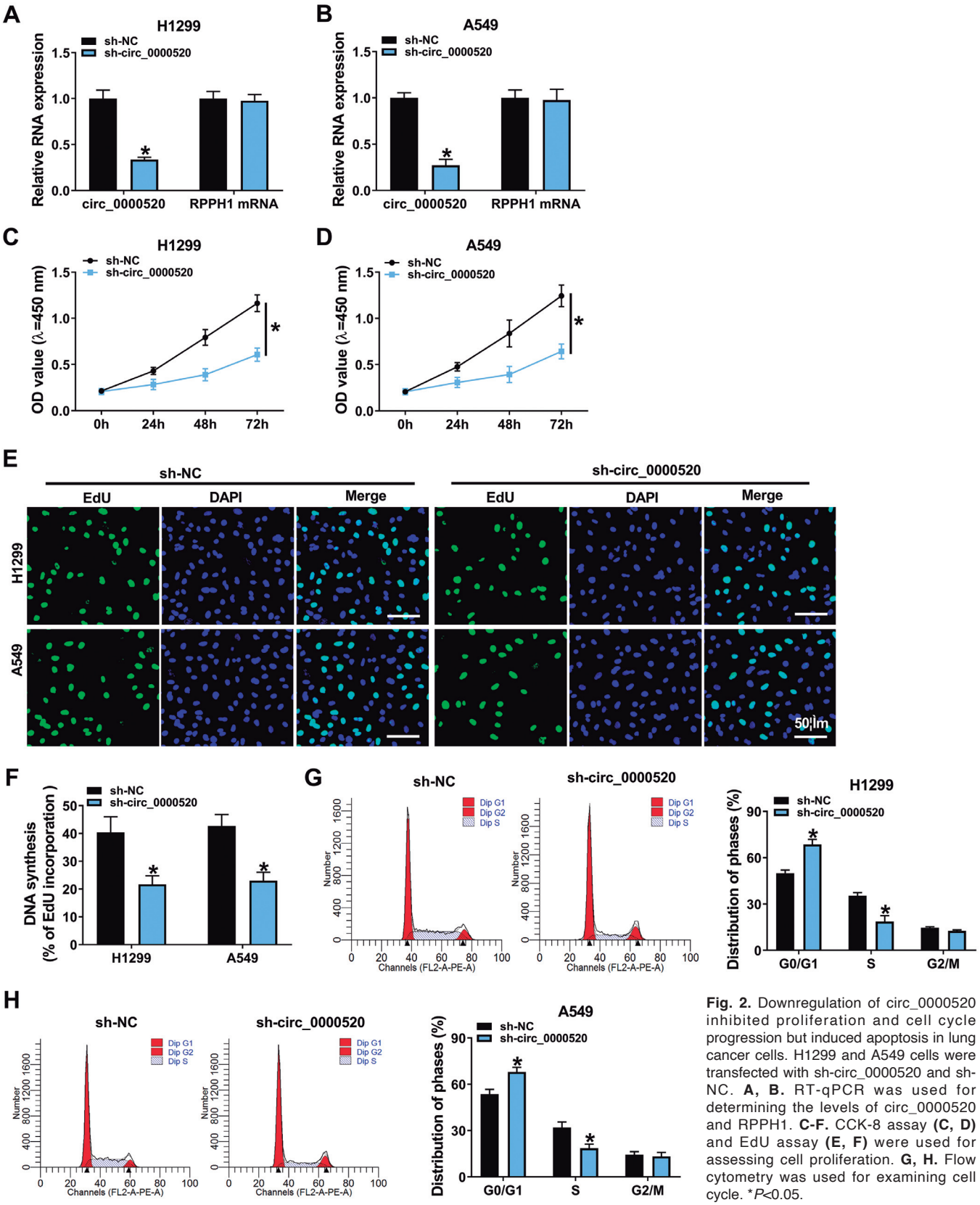

Fig. 2. Downregulation of circ_0000520 inhibited proliferation and cell cycle progression but induced apoptosis in lung cancer cells. H1299 and A549 cells were transfected with sh-circ_0000520 and sh-NC. **A, B.** RT-qPCR was used for determining the levels of circ_0000520 and RPPH1. **C-F.** CCK-8 assay **(C, D)** and EdU assay **(E, F)** were used for assessing cell proliferation. **G, H.** Flow cytometry was used for examining cell cycle. **P*<0.05.

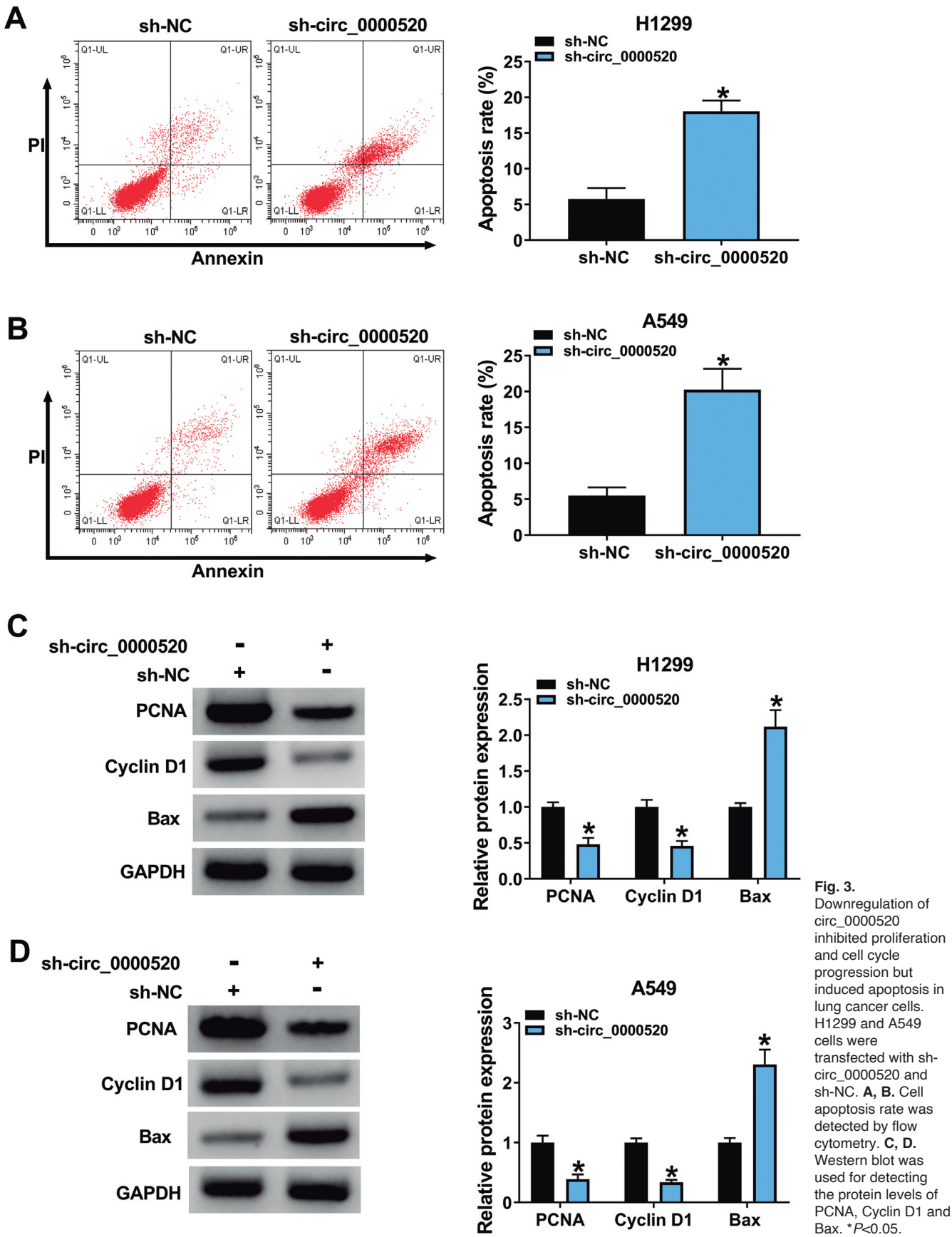

Fig. 3. Downregulation of circ_0000520 inhibited proliferation and cell cycle progression but induced apoptosis in lung cancer cells. H1299 and A549 cells were transfected with sh-circ_0000520 and sh-NC. **A, B.** Cell apoptosis rate was detected by flow cytometry. **C, D.** Western blot was used for detecting the protein levels of PCNA, Cyclin D1 and Bax. **P*<0.05.

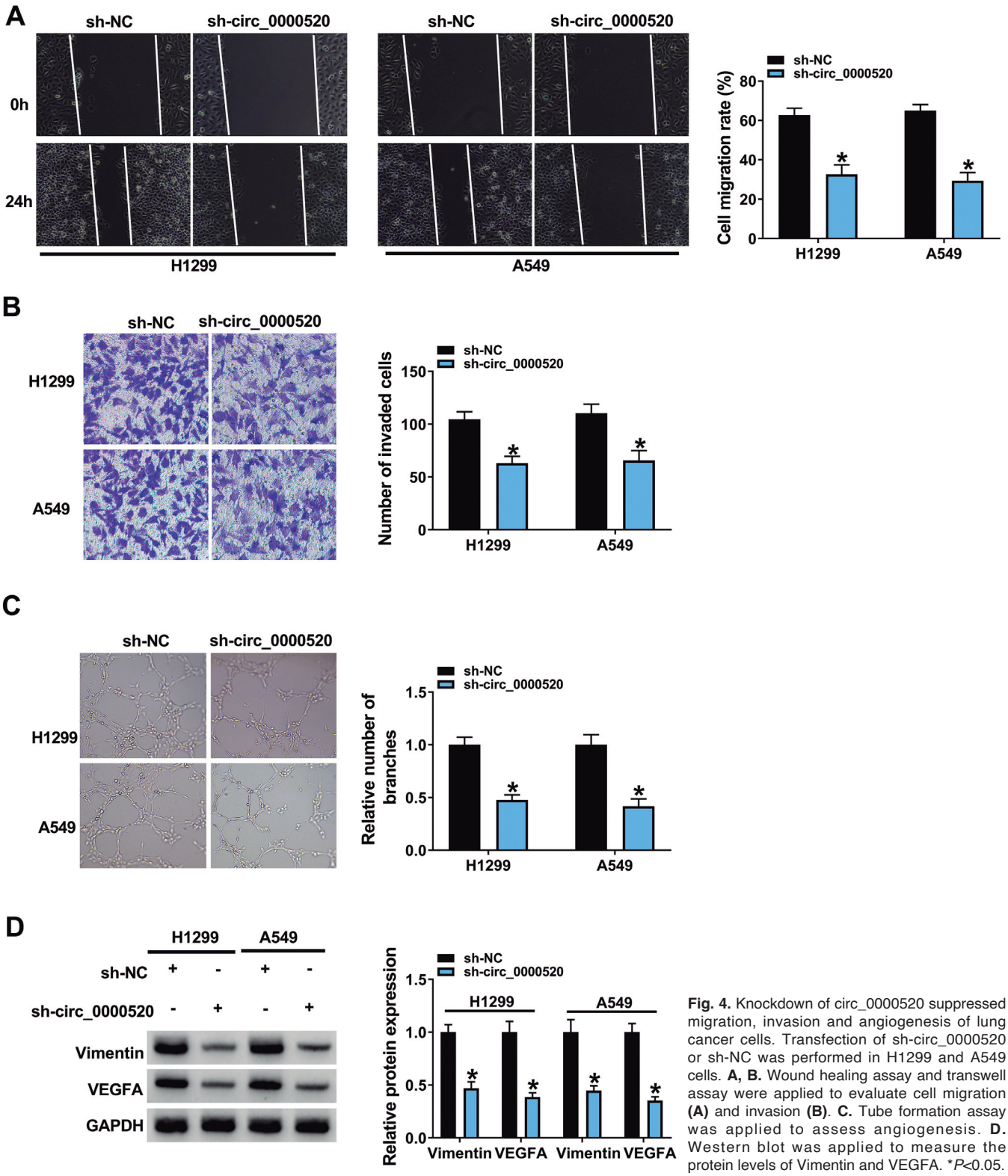

Fig. 4. Knockdown of circ_0000520 suppressed migration, invasion and angiogenesis of lung cancer cells. Transfection of sh-circ_0000520 or sh-NC was performed in H1299 and A549 cells. **A, B.** Wound healing assay and transwell assay were applied to evaluate cell migration **(A)** and invasion **(B)**. **C.** Tube formation assay was applied to assess angiogenesis. **D.** Western blot was applied to measure the protein levels of Vimentin and VEGFA. **P*<0.05.

prevented the transition from G0/G1 phase to S phase (Fig. 2G,H) and enhanced cell apoptosis rate (Fig. 3A,B) in H1299 and A549 cells. Moreover, the protein markers were examined by western blot. The protein downregulation of PCNA and Cyclin D1 as well as the upregulation of Bax demonstrated that silence of circ_0000520 repressed lung cancer cell growth and promoted apoptosis (Fig. 3C,D). These results demonstrated that circ_0000520 promoted lung cancer cell progression.

Knockdown of circ_0000520 suppressed migration, invasion and angiogenesis of lung cancer cells

Then, the effects of circ_0000520 on cell metastasis and angiogenesis were assessed. Wound healing assay and transwell assay exhibited that the migration rate (Fig. 4A) and invaded cell number (Fig. 4B) were significantly decreased, as a result of circ_0000520 knockdown. The data from tube formation assay suggested that circ_0000520 level inhibition attenuated the angiogenetic ability of HUVECs after co-culture with H1299 and A549 cells (Fig. 4C). Also, circ_0000520 knockdown downregulated the protein levels of Vimentin and VEGFA (Fig. 4D). These data validated that circ_0000520 promoted metastatic and angiogenetic capacities in lung cancer cells.

Circ_0000520 contributed to tumor growth of lung cancer in vivo

The function of circ_0000520 in regulating tumorigenesis was explored by xenograft tumor assay. Tumor volume (Fig. 5A) and weight (Fig. 5B,C) were obviously lower in sh-circ_0000520 than those in sh-NC group. RT-qPCR detection in tumor tissues showed that circ_0000520 was downregulated by sh-circ_0000520 (Fig. 5D). IHC assay also demonstrated that downregulation of circ_0000520 inhibited the protein expression of Ki67 in tissues (Fig. 5E). Hence, tumor growth of lung cancer was enhanced by circ_0000520 *in vivo*.

Circ_0000520 exerted a sponge influence on miR-512-5p

Three miRNAs (miR-1233-3p, miR-1296-5p, miR-512-5p) were commonly predicted as the targets of circ_0000520 by circbank and circinteractome (Fig. 6A). Subsequently, our expression detection indicated that miR-512-5p was upregulated with the most conspicuous change after circ_0000520 downregulation in H1299 and A549 cells (Fig. 6B). The binding sites between circ_0000520 and miR-512-5p are displayed as Fig. 6C. In comparison with miR-NC and anti-NC groups, miR-512-5p level was markedly increased by miR-512-5p transfection but downregulated by anti-miR-512-5p transfection (Fig. 6D). The relative luciferase activity was found to be suppressed after co-transfection with miR-512-5p and WT-circ_0000520 rather than miR-512-5p and MUT-circ_0000520 in H1299 and A549 cells (Fig. 6E-F). The expression reduction of miR-512-5p was detected in lung cancer tissues compared with normal tissues (Fig. 6G), and circ_0000520 exhibited a negative relation (r=-0.5802, P<0.0001) with miR-512-5p (Fig. 6H). Also, miR-512-5p was downregulated in H1299 and A549 cells compared to 16HBE cells (Fig. 6I). Then, anti-miR-512-5p reversed the promoting

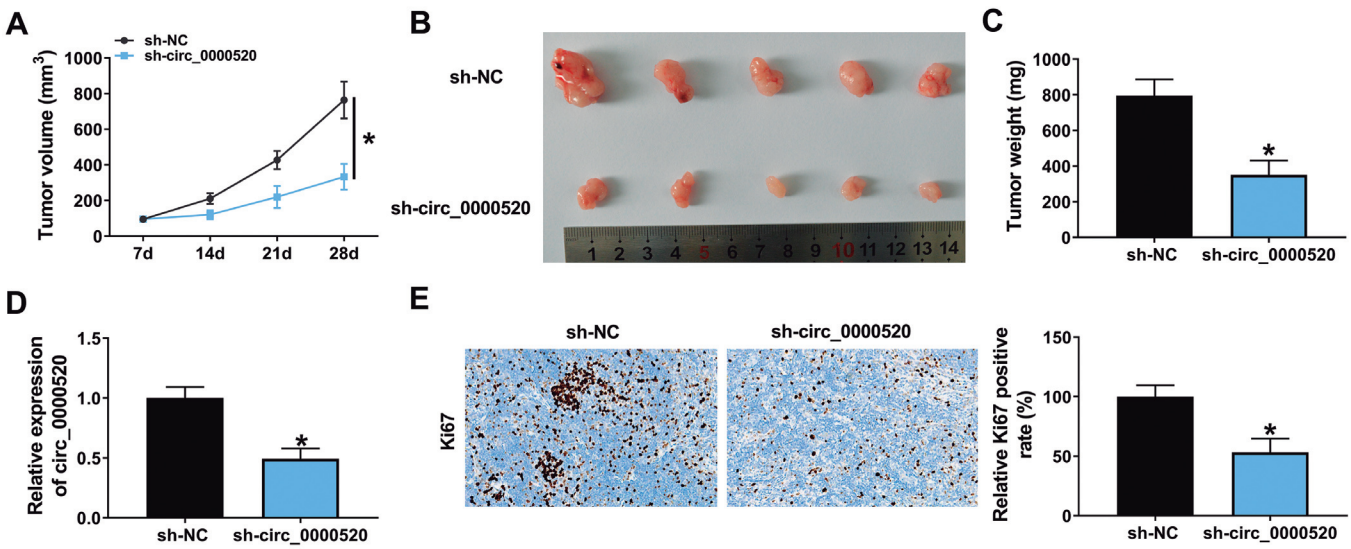

Fig. 5. Circ_0000520 contributed to tumor growth of lung cancer in vivo. **A.** Tumor volume was determined in sh-NC and sh-circ_0000520 groups of mice. **B.** Tumor images of all mice in two groups. **C.** The weight was measured in each group. **D.** The circ_0000520 was quantified by RT-qPCR in tumor tissues. **E.** Ki67 detection was performed using IHC assay. *P<0.05.

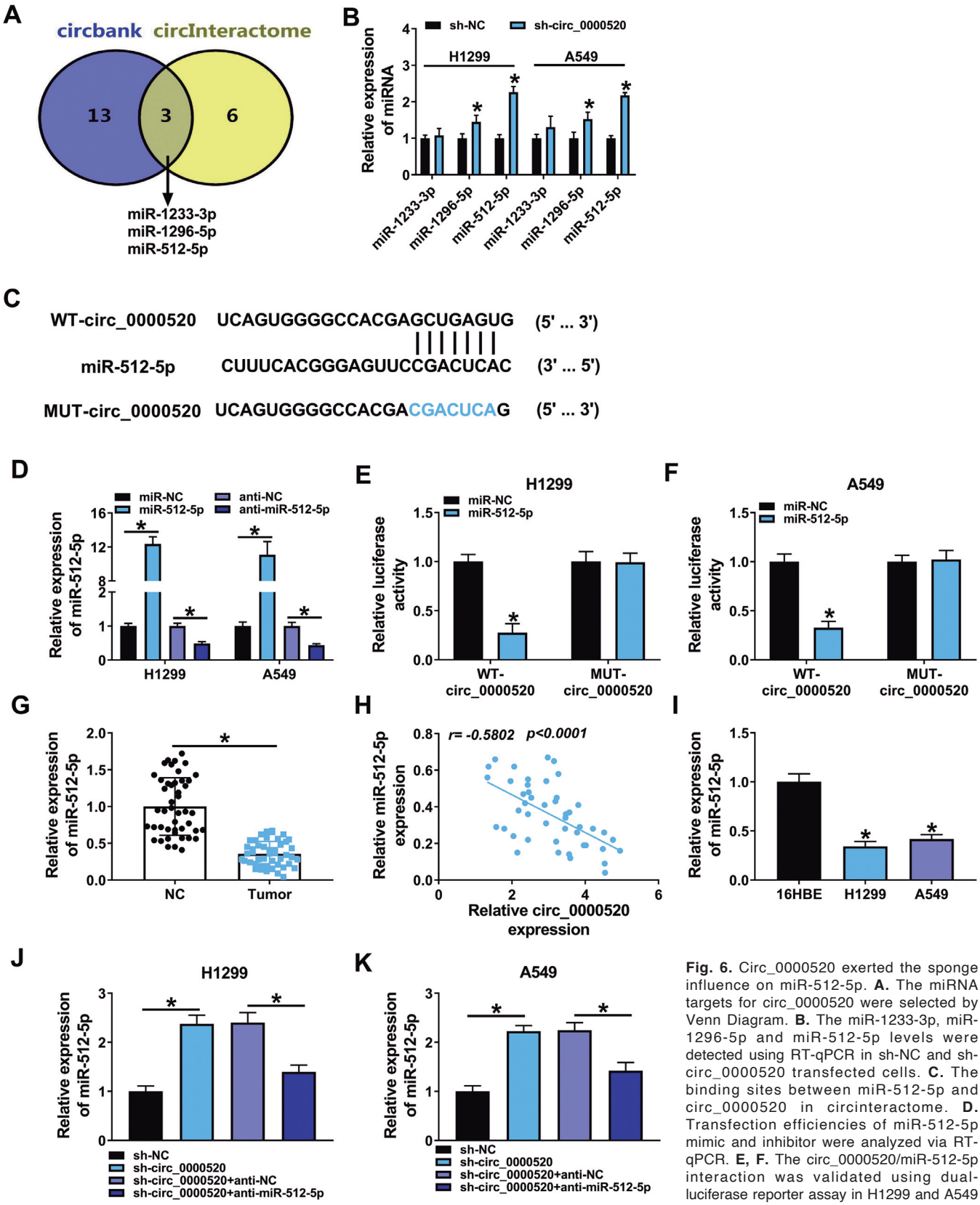

Fig. 6. Circ_0000520 exerted the sponge influence on miR-512-5p. **A.** The miRNA targets for circ_0000520 were selected by Venn Diagram. **B.** The miR-1233-3p, miR-1296-5p and miR-512-5p levels were detected using RT-qPCR in sh-NC and sh-circ_0000520 transfected cells. **C.** The binding sites between miR-512-5p and circ_0000520 in circinteractome. **D.** Transfection efficiencies of miR-512-5p mimic and inhibitor were analyzed via RT-qPCR. **E, F.** The circ_0000520/miR-512-5p interaction was validated using dual-luciferase reporter assay in H1299 and A549 cells. **G.** The miR-512-5p quantification was conducted by RT-qPCR in lung cancer tissues. **H.** Pearson's correlation coefficient was used for linear analysis between circ_0000520 and miR-512-5p. **I.** The miR-512-5p level was assayed via RT-qPCR in H1299 and A549 cells. **J, K.** RT-qPCR was performed for miR-512-5p level analysis in sh-circ_0000520, sh-circ_0000520+anti-miR-512-5p or the negative control groups. **P*<0.05.

effect of sh-circ_0000520 on miR-512-5p level in H1299 and A549 cells (Fig. 6J,K). Taken together, circ_0000520 targeted miR-512-5p to inhibit miR-512-5p expression in lung cancer cells.

The anti-tumor function by circ_0000520 knockdown was attenuated after the downregulation of miR-512-5p

Furthermore, we investigated the circ_0000520/miR-512-5p axis in cell function regulation. Cell proliferation inhibition (Fig. 7A-C), cell cycle arrest (Fig. 7D,E) and apoptosis promotion (Fig. 7F) caused by sh-circ_0000520 were significantly relieved after miR-512-5p level was reduced in H1299 and A549 cells. Western blot analysis suggested that miR-512-5p inhibitor eliminated the effects of sh-circ_0000520 on PCNA, Cyclin D1 and Bax proteins (Fig. 8A,B). The sh-circ_0000520-induced suppression of migration (Fig. 8C), invasion (Fig. 8D) and angiogenesis (Fig. 8E) was also abolished by anti-miR-512-5p. Meanwhile,

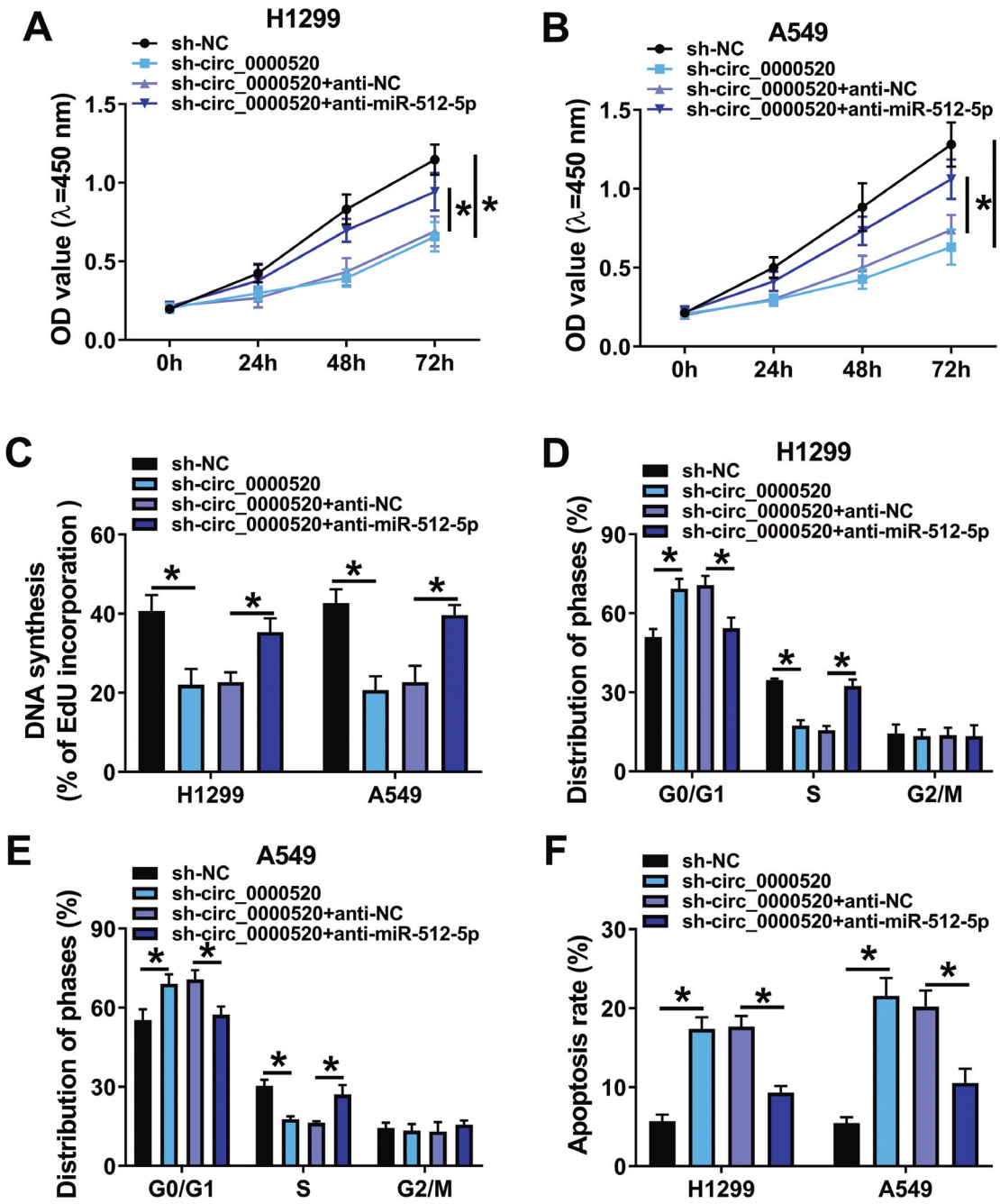

Fig. 7. The anti-tumor function by circ_0000520 knockdown was attenuated after the downregulation of miR-512-5p. H1299 and A549 cells were transfected with sh-NC, sh-circ_0000520, sh-circ_0000520+anti-NC, and sh-circ_0000520+anti-miR-512-5p. **A-C.** The proliferation detection was conducted through CCK-8 assay **(A, B)** and EdU assay **(C)**. **D-F.** Cell cycle **(D, E)** and apoptosis **(F)** were examined through flow cytometry. **P*<0.05.

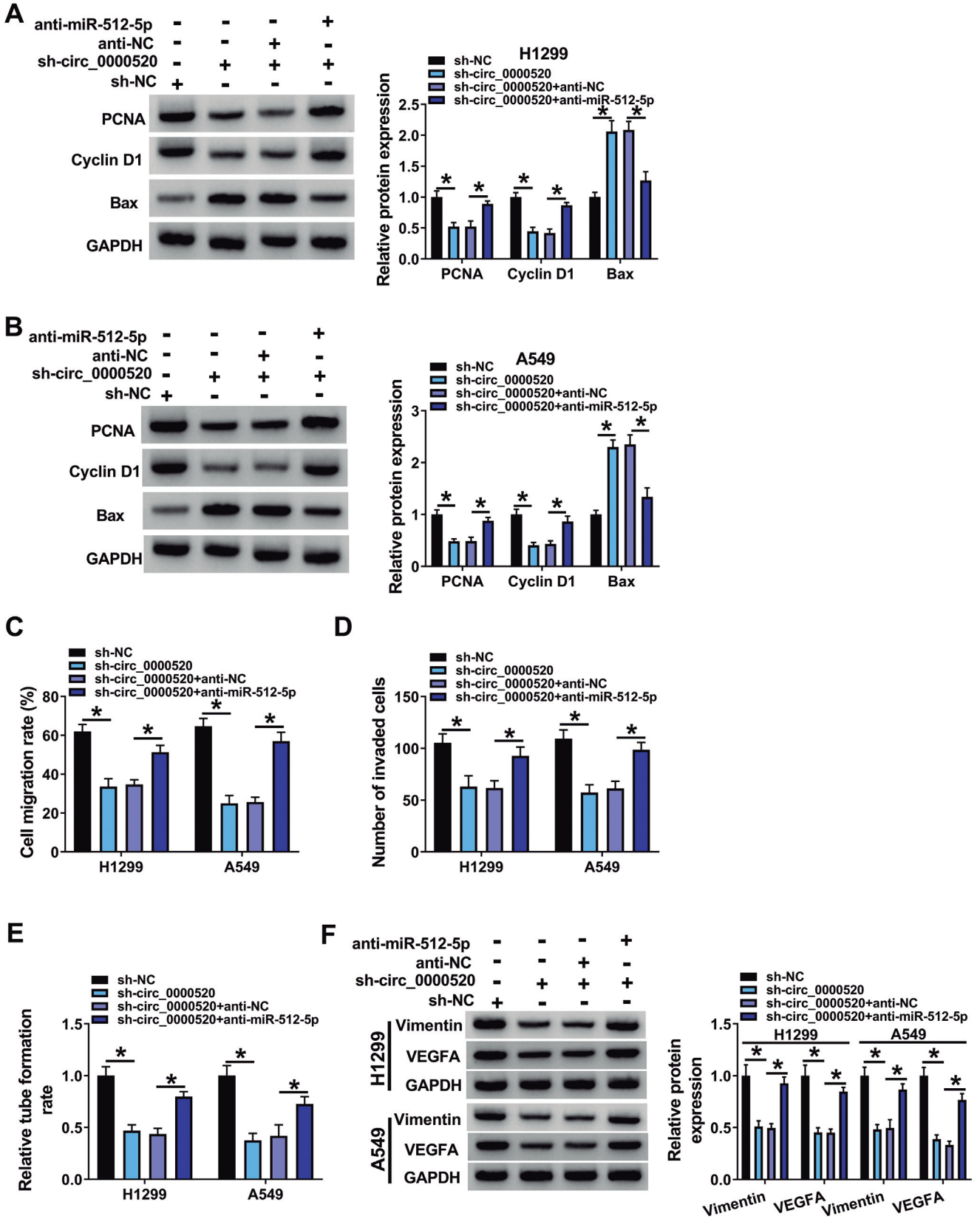

Fig. 8. The anti-tumor function by circ_0000520 knockdown was attenuated after the downregulation of miR-512-5p. H1299 and A549 cells were transfected with sh-NC, sh-circ_0000520, sh-circ_0000520+anti-NC, and sh-circ_0000520+anti-miR-512-5p. **A, B.** The protein analysis of PCNA, Cyclin D1 and Bax was conducted through western blot. **C, D.** The assessment of migration **(C)** and invasion **(D)** was conducted through wound healing assay and transwell assay. **E.** The angiogenesis examination was performed via tube formation assay. **F.** Vimentin and VEGFA protein quantification was performed via western blot. **P*<0.05.

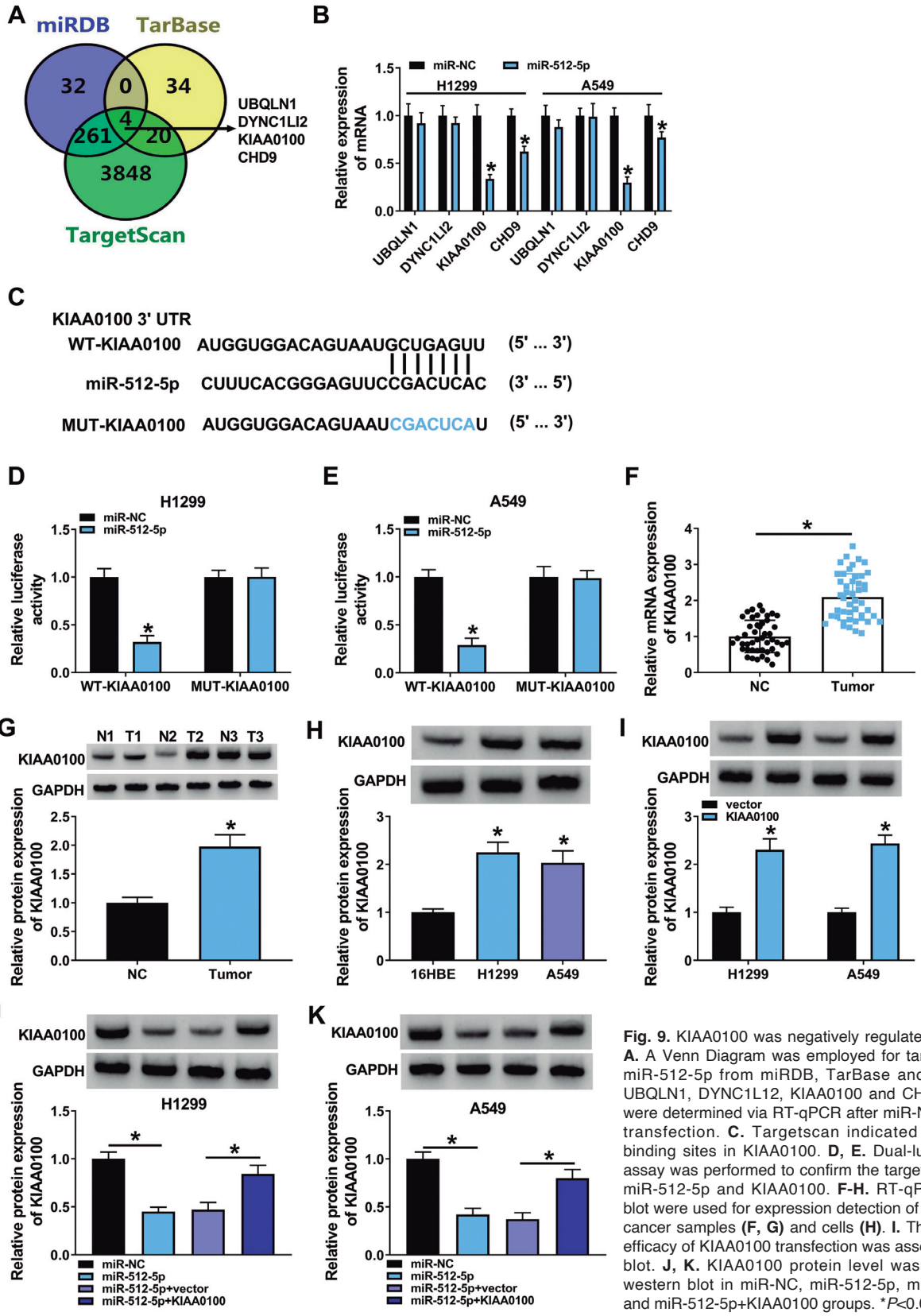

Fig. 9. KIAA0100 was negatively regulated by miR-512-5p. **A.** A Venn Diagram was employed for target screening for miR-512-5p from miRDB, TarBase and Targetscan. **B.** UBQLN1, DYNC1L12, KIAA0100 and CHD9 mRNA levels were determined via RT-qPCR after miR-NC or miR-512-5p transfection. **C.** Targetscan indicated the miR-512-5p binding sites in KIAA0100. **D, E.** Dual-luciferase reporter assay was performed to confirm the target binding between miR-512-5p and KIAA0100. **F-H.** RT-qPCR and western blot were used for expression detection of KIAA0100 in lung cancer samples **(F, G)** and cells **(H)**. **I.** The overexpression efficacy of KIAA0100 transfection was assessed via western blot. **J, K.** KIAA0100 protein level was examined using western blot in miR-NC, miR-512-5p, miR-512-5p+vector and miR-512-5p+KIAA0100 groups. **P*<0.05.

Vimentin and VEGFA protein levels were upregulated in sh-circ_0000520+anti-miR-512-5p group compared with sh-circ_0000520+anti-NC group (Fig. 8F). Overall, the regulatory function of circ_0000520 was related to the direct miR-512-5p downregulation.

KIAA0100 was negatively regulated by miR-512-5p

Targetscan, TarBase and miRDB predicted that UBQLN1, DYNC1L12, KIAA0100 and CHD9 might be the targets of miR-512-5p (Fig. 9A). The inhibitory effect of miR-512-5p on KIAA0100 mRNA expression was the most significant in H1299 and A549 cells (Fig. 9B). KIAA0100 3'UTR sequence contained the complementary sites of miR-512-5p (Fig. 9C), and dual-luciferase reporter assay demonstrated that miR-512-5p could bind to KIAA0100 to inhibit the luciferase activity of WT-KIAA0100 group (Fig. 9D,E). RT-qPCR and western blot assays showed that KIAA0100 was upregulated in lung cancer tissues (Fig. 9F,G) and cells

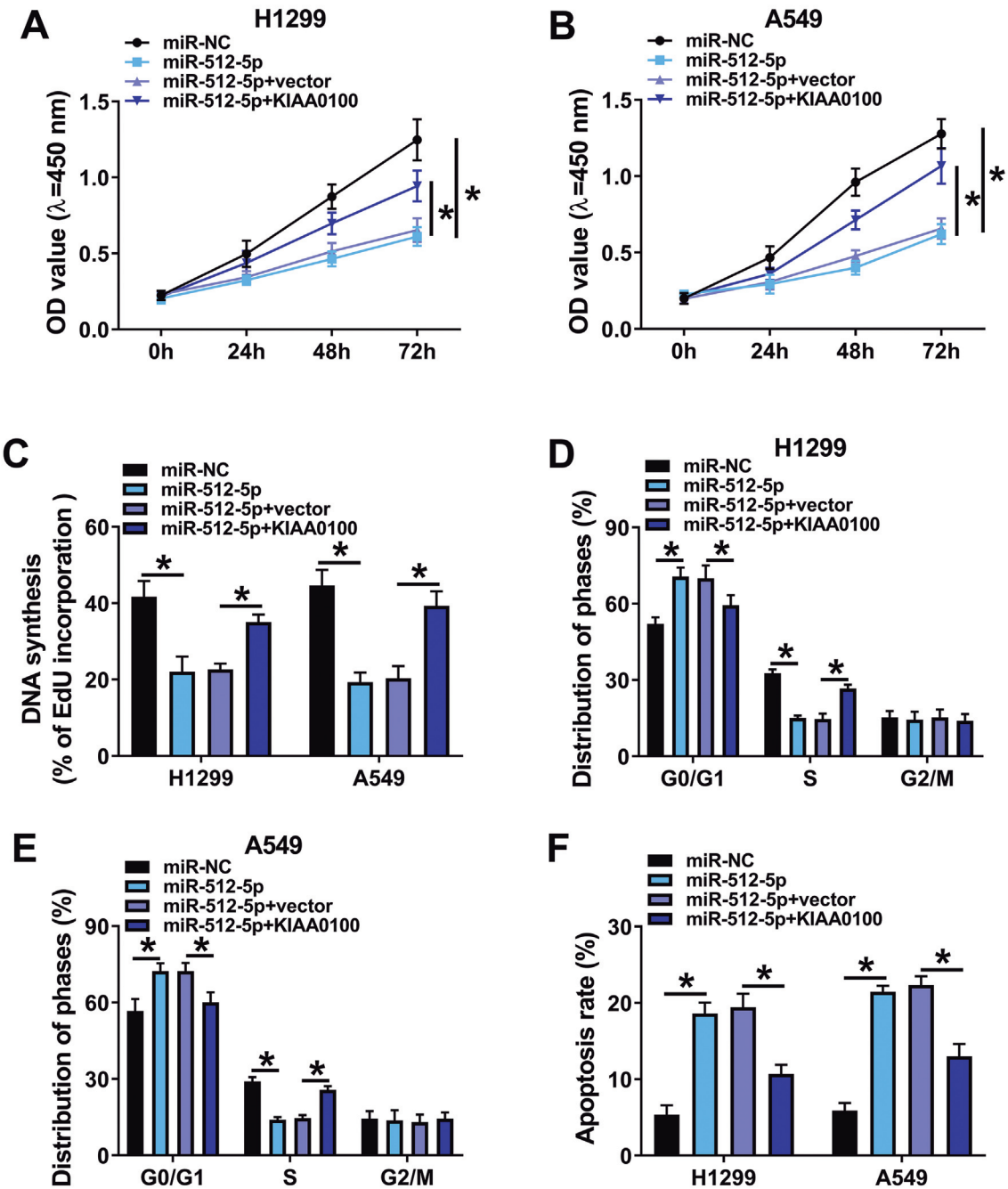

Fig. 10. miR-512-5p downregulated KIAA0100 to act as a tumor inhibitor in lung cancer. H1299 and A549 cells were conducted with transfection of miR-NC, miR-512-5p, miR-512-5p+vector and miR-512-5p+KIAA0100. **A-C.** Cell proliferation ability was analyzed via CCK-8 assay **(A, B)** and EdU assay **(C)**. **D-F.** Cell cycle progression **(D, E)** and apoptosis rate **(F)** were measured via flow cytometry. **P*<0.05.

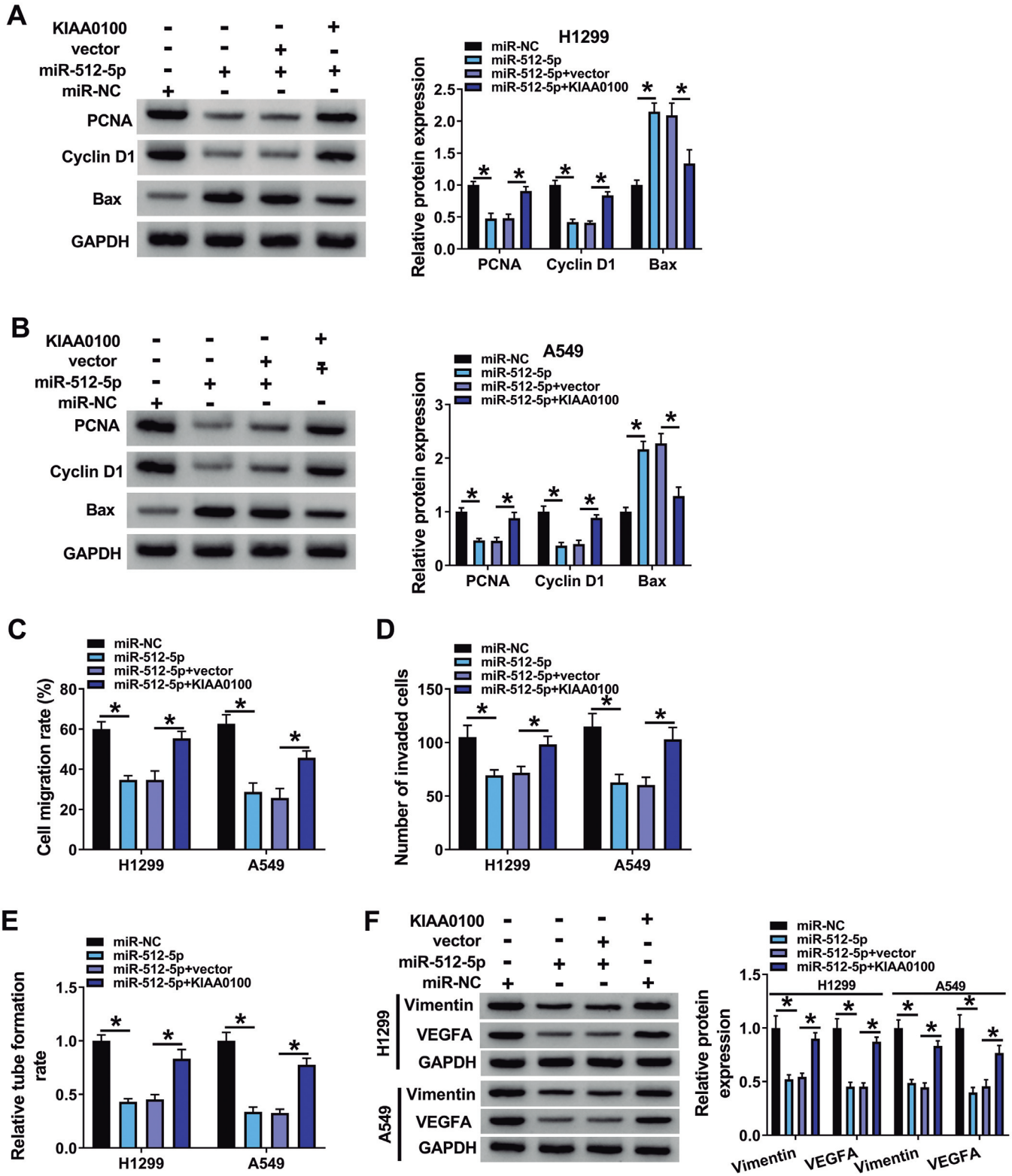

Fig. 11. miR-512-5p downregulated KIAA0100 to act as a tumor inhibitor in lung cancer. H1299 and A549 cells were conducted with transfection of miR-NC, miR-512-5p, miR-512-5p+vector and miR-512-5p+KIAA0100. **A, B.** PCNA, Cyclin D1 and Bax levels were detected via western blot. **C, D.** Cell migration **(C)** and invasion **(D)** were assessed via wound healing assay and transwell assay. **E.** Tube formation ability was evaluated via tube formation assay. **F.** Vimentin and VEGFA protein levels were examined through western blot. **P*<0.05.

(Fig. 9H). KIAA0100 overexpression was achieved by transfection of KIAA0100 in H1299 and A549 cells, relative to vector transfection (Fig. 9I). The protein level of KIAA0100 was decreased by miR-512-5p mimic, which was counteracted by KIAA0100 transfection (Fig. 9J-K). Indeed, miR-512-5p was able to induce the direct downregulation of KIAA0100.

The miR-512-5p downregulated KIAA0100 acts as a tumor inhibitor in lung cancer

The influences of miR-512-5p and KIAA0100 on the malignant behaviors of lung cancer cells were further researched. Overexpression of miR-512-5p was shown to inhibit cell proliferation (Fig. 10A-C) and cell cycle progression (Fig. 10D,E) but accelerated cell apoptosis (Fig. 10F) in H1299 and A549 cells, then KIAA0100 upregulation abrogated these effects. KIAA0100 transfection also abated the regulation of miR-512-5p in protein expression of PCNA, Cyclin D1 and Bax (Fig. 11A,B). Cell migration rate (Fig. 11C), invasion ability (Fig. 11D) and tube formation ability (Fig. 11E) were all suppressed by miR-512-5p by inducing the inhibition of KIAA0100. The introduction of KIAA0100 also lightened the miR-512-5p-induced protein down-regulation of Vimentin and VEGFA (Fig. 11F). Thus, miR-512-5p inhibited tumor progression of lung cancer cells by targeting KIAA0100.

Circ_0000520 regulated KIAA0100 via interacting with miR-512-5p

RT-qPCR and western blot were used for detecting the KIAA0100 expression by the circ_0000520/miR-512-5p axis. The results showed that circ_0000520 knockdown inhibited the mRNA and protein levels of KIAA0100 in H1299 (Fig. 12A,B) and A549 (Fig. 12C,D) cells, whereas anti-miR-512-5p mitigated this regulation. The above evidence identified the positive effect of circ_0000520 on KIAA0100 level via targeting miR-512-5p.

Discussion

Previous studies have shown that circ_0000520 played a oncogenic role in cancer biology (Shang et al., 2016; Ruan et al., 2020). In this study, we confirmed that circ_0000520 promoted cell malignant phenotypes of lung cancer by affecting the miR-512-5p/KIAA0100 network.

Our circRNA screening analysis identified that circ_0000520 was aberrantly upregulated in lung cancer. With the improvement of molecular technology, increasing dysregulated circRNAs were found to act as oncogenes or inhibitors in the progression of human cancers. Wang et al. showed that circRNA_10156 facilitated proliferation capacity of hepatitis B virus-

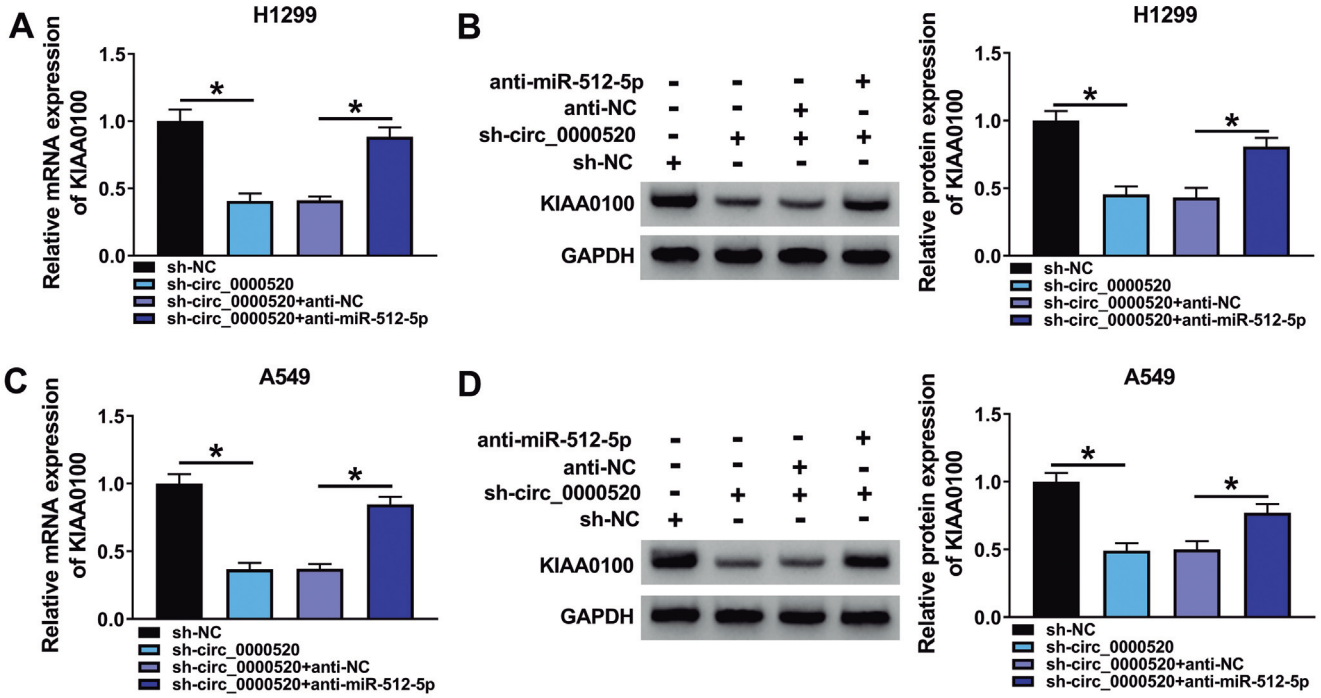

Fig. 12. Circ_0000520 regulated KIAA0100 by interacting with miR-512-5p. **A-D.** The mRNA and protein levels of KIAA0100 were assayed by RT-qPCR and western blot after sh-NC, sh-circ_0000520, sh-circ_0000520+anti-NC, or sh-circ_0000520+anti-miR-512-5p transfection in H1299 **(A, B)** and A549 **(C, D)** cells. **P*<0.05.

induced liver cancer (Wang et al., 2020a; Chen et al., 2019) elucidated that circRNA_0000285 resulted in pro-tumorigenic function in cervical cancer (Chen et al., 2019). CircRNA-000911 restrained cell invasion and evoked apoptosis in breast cancer (Wang et al., 2018), and the enhanced level of circHIPK3 impeded the biological behaviors of ovarian cancer cells (Teng et al., 2019). By performing cellular experiments, circ_0000520 downregulation was shown to trigger proliferation inhibition, cell cycle retardation and apoptosis enhancement. Additionally, cell motility and angiogenesis were significantly suppressed after circ_0000520 level was silenced in lung cancer cells. Moreover, interfering circ_0000520 reduced tumor growth in mice. The collective data revealed that circ_0000520 was an oncogenic RNA in lung cancer progression. miR-512-5p was predicted as a miRNA target for circ_0000520, and the sponge effect of circ_0000520 on miR-512-5p was validated in lung cancer cells. The miRNA sponging function is one of the most important mechanisms of circRNA regulation in different cancer types. Shi et al. showed that circLPAR3 accelerated migration and metastasis in esophageal cancer via sponging miR-198 (Shi et al., 2020; Wei et al., 2020) discovered that silencing circRNA_104433 led to cell growth inhibition of gastric cancer through targeting miR-497-5p (Wei et al., 2020). Also, circ-SLC7A6 sponged miR-21 to induce the tumor-suppressive regulation in lung cancer development (Wang et al., 2020b). The current results show that sh-circ_0000520-mediated cancer progression inhibition was restored by miR-512-5p inhibitor, which implied that circ_0000520 exerted a tumorigenic role in lung cancer partly via sequestering miR-512-5p.

Subsequently, we selected KIAA0100 as a target molecule downstream of miR-512-5p and affirmed the miR-512-5p/KIAA0100 target relation. In addition, miR-512-5p expression activation incurred Mcl-1 downregulation to promote gastric cancer cell apoptosis (Saito et al., 2009). Herein, miR-512-5p overexpression suppressed the malignant behaviors in lung cancer cells via through inhibitory effect on KIAA0100 level. KIAA0100 acted as an oncogene in lung cancer.

More importantly, we noticed that circ_0000520 knockdown downregulated KIAA0100 expression by releasing miR-512-5p. CircRNA_103809 contributed to lung cancer development by competitively interacting with miR-4302 to induce the ZNF121-related MYC upregulation (Liu et al., 2018). CircSMARCA5 limited cell progression through miR-670-5p-dependent RBM24 regulation in lung cancer (Zhang et al., 2020). Thus, circ_0000520 was considered to facilitate lung cancer progression by influencing the miR-512-5p/KIAA0100 axis.

Conclusion

In conclusion, circ_0000520 was associated with malignant development in lung cancer partly by depending on the miR-512-5p/KIAA0100 network. The Circ_0000520/miR-512-5p/KIAA0100 axis was a novel molecular mechanism involved in the progression of lung cancer.

Conflicts of interest. The authors have no conflict of interest to declare.

Data Availability Statement. The datasets used and analyzed during the current study are available from the corresponding author on reasonable request.

Funding. This study was supported by Medical discipline Construction Project of Pudong Health Committee of Shanghai (Grant No. PWYst2021-18) and the Key discipline construction project of pPudongHealth Bureau of Shanghai (PWZxk2017-24).

References

Chen R.X., Liu H.L., Yang L.L., Kang F.H., Xin L.P., Huang L.R., Guo Q.F. and Wang Y.L. (2019). Circular RNA circRNA_0000285 promotes cervical cancer development by regulating FUS. Eur. Rev. Med. Pharmacol. Sci. 23, 8771-8778.

Chu K., Gao G., Yang X., Ren S., Li Y., Wu H., Huang Y. and Zhou C. (2016). MiR-512-5p induces apoptosis and inhibits glycolysis by targeting p21 in non-small cell lung cancer cells. Int. J. Oncol. 48, 577-586.

Drula R., Braicu C., Harangus A., Nabavi S.M., Trif M., Slaby O., Ionescu C., Irimie A. and Berindan-Neagoe I. (2020). Critical function of circular RNAs in lung cancer. Wiley Interdiscip Rev. RNA 11, e1592.

Guo J., Wang M. and Liu X. (2015). MicroRNA-195 suppresses tumor cell proliferation and metastasis by directly targeting BCOX1 in prostate carcinoma. J. Exp. Clin. Cancer Res. 34, 91.

Halliday P.R., Blakely C.M. and Bivona T.G. (2019). Emerging targeted therapies for the treatment of non-small cell lung cancer. Curr. Oncol. Rep. 21, 21.

Li J., Lei H., Xu Y. and Tao Z.Z. (2015). miR-512-5p suppresses tumor growth by targeting hTERT in telomerase positive head and neck squamous cell carcinoma in vitro and in vivo. PLoS One 10, e0135265.

Li B., Wang Z., Yang F., Huang J., Hu X., Deng S., Tian M. and Si X. (2021). miR449a5p suppresses CDK6 expression to inhibit cardiomyocyte proliferation. Mol. Med. Rep. 23, 14.

Liu T., Zhang X.Y., He X.H., Geng J.S., Liu Y., Kong D.J., Shi Q.Y., Liu F., Wei W. and Pang D. (2014). High levels of BCOX1 expression are associated with poor prognosis in patients with invasive ductal carcinomas of the breast. PLoS One 9, e86952.

Liu W., Ma W., Yuan Y., Zhang Y. and Sun S. (2018). Circular RNA hsa_circRNA_103809 promotes lung cancer progression via facilitating ZNF121-dependent MYC expression by sequestering miR-4302. Biochem. Biophys. Res. Commun. 500, 846-851.

Livak K.J. and Schmittgen T.D. (2001). Analysis of relative gene expression data using real-time quantitative PCR and the 2(-Delta Delta C(T)) Method. Methods 25, 402-408.

Nooreldeen R. and Bach H. (2021). Current and future development in lung cancer diagnosis. Int. J. Mol. Sci. 22, 8661.

Panda A.C. (2018). Circular RNAs act as miRNA sponges. Adv. Exp. Med. Biol. 1087, 67-79.

Ruan Y., Li Z., Shen Y., Li T., Zhang H. and Guo J. (2020). Functions of circular RNAs and their potential applications in gastric cancer.

Expert Rev. Gastroenterol. Hepatol. 14, 85-92.

Saito Y., Suzuki H., Tsugawa H., Nakagawa I., Matsuzaki J., Kanai Y. and Hibi T. (2009). Chromatin remodeling at Alu repeats by epigenetic treatment activates silenced microRNA-512-5p with downregulation of Mcl-1 in human gastric cancer cells. Oncogene 28, 2738-2744.

Shang X., Li G., Liu H., Li T., Liu J., Zhao Q. and Wang C. (2016). Comprehensive circular RNA profiling reveals that hsa_circ_0005075, a new circular RNA biomarker, is involved in hepatocellular carcinoma development. Medicine (Baltimore) 95, e3811.

Shi Y., Fang N., Li Y., Guo Z., Jiang W., He Y., Ma Z. and Chen Y. (2020). Circular RNA LPAR3 sponges microRNA-198 to facilitate esophageal cancer migration, invasion, and metastasis. Cancer Sci. 111, 2824-2836.

Sun H., Tang W., Rong D., Jin H., Fu K., Zhang W., Liu Z., Cao H. and Cao X. (2018). Hsa_circ_0000520, a potential new circular RNA biomarker, is involved in gastric carcinoma. Cancer Biomark. 21, 299-306.

Sun J., Xin K., Leng C. and Ge J. (2021). Down-regulation of SNHG16 alleviates the acute lung injury in sepsis rats through miR-128-3p/HMGB3 axis. BMC Pulm. Med. 21, 191.

Teng F., Xu J., Zhang M., Liu S., Gu Y., Zhang M., Wang X., Ni J., Qian B., Shen R. and Jia X. (2019). Comprehensive circular RNA expression profiles and the tumor-suppressive function of circHIPK3 in ovarian cancer. Int. J. Biochem. Cell Biol. 112, 8-17.

Thai A.A., Solomon B.J., Sequist L.V., Gainor J.F. and Heist R.S. (2021). Lung cancer. Lancet 398, 535-554.

Wang H., Xiao Y., Wu L. and Ma D. (2018). Comprehensive circular RNA profiling reveals the regulatory role of the circRNA-000911/miR-449a pathway in breast carcinogenesis. Int. J. Oncol. 52, 743-754.

Wang M., Gu B., Yao G., Li P. and Wang K. (2020a). Circular RNA expression profiles and the pro-tumorigenic function of CircRNA_10156 in hepatitis B virus-related liver cancer. Int. J. Med. Sci. 17, 1351-1365.

Wang Y., Zheng F., Wang Z., Lu J. and Zhang H. (2020b). Circular RNA circ-SLC7A6 acts as a tumor suppressor in non-small cell lung cancer through abundantly sponging miR-21. Cell Cycle 19, 2235-2246.

Wang Z., Zhu X., Zhang T. and Yao F. (2020c). miR-512-5p suppresses the progression of non-small cell lung cancer by targeting beta-catenin. Oncol. Lett. 19, 415-423.

Wei W., Mo X., Yan L., Huang M., Yang Y., Jin Q., Zhong H., Cao W., Wu K., Wu L., Li Z., Wang T., Qin Y. and Chen J. (2020). Circular RNA profiling reveals that circRNA_104433 regulates cell growth by targeting miR-497-5p in gastric cancer. Cancer Manag. Res. 12, 15-30.

Xie S., Wu Z., Qi Y., Wu B. and Zhu X. (2021). The metastasizing mechanisms of lung cancer: Recent advances and therapeutic challenges. Biomed. Pharmacother. 138, 111450.

Zarredar H., Ansarin K., Baradaran B., Shekari N., Eyvazi S., Safari F. and Farajnia S. (2018). Critical microRNAs in lung cancer: Recent advances and potential applications. Anticancer Agents Med. Chem. 18, 1991-2005.

Zhang D., Ma Y., Ma Z., Liu S., Sun L., Li J., Zhao F., Li Y., Zhang J., Li S. and Jiang J. (2020). Circular RNA SMARCA5 suppressed non-small cell lung cancer progression by regulating miR-670-5p/RBM24 axis. Acta Biochim. Biophys. Sin. (Shanghai) 52, 1071-1080.

Zheng Q., Zhang J., Zhang T., Liu Y., Du X., Dai X. and Gu D. (2021). Hsa_circ_0000520 overexpression increases CDK2 expression via miR-1296 to facilitate cervical cancer cell proliferation. J. Transl. Med. 19, 314.

Zhou Y., Ma G., Peng S., Tuo M., Li Y., Qin X., Yu Q., Kuang S., Cheng H. and Li J. (2021). Circ_0000520 contributes to triple-negative breast cancer progression through mediating the miR-1296/ZFX axis. Thorac. Cancer 12, 2427-2438.

Accepted July 22, 2022